Trapping Effects in the Transient Response of AlGaN/GaN HEMT Devices

José María Tirado, José Luis Sánchez-Rojas, and José Ignacio Izpura

***Abstract*—In this paper, the transient analysis of an AlGaN/GaN high-electron mobility transistor (HEMT) device is presented. Drain–current dispersion effects are investigated when gate or drain voltages are pulsed. Gate-lag and drain-lag turn-on measurements are analyzed, revealing clear mechanisms of current collapse and related dispersion effects. Numerical 2-D transient simulations considering surface traps effects in a physical HEMT model have also been carried out. A comparison between experimental and theoretical results is shown. The presence of donor-type traps acting as hole traps, due to their low energy level of 0.25 eV relative to the valence band, with densities $>$ 1e20 cm^{-3} ($>$ 5e12 cm^{-2}), uniformly distributed at the HEMT surface, and interacting with the free holes that accumulated at the top surface due to piezoelectric fields, accounts for the experimentally observed effects. Time constants next to 10 ms are deduced. Some additional features in the measured transient currents, with faster time constants, could not be associated with surface states.**

***Index Terms*—AlGaN/GaN high-electron mobility transistor (HEMT), current collapse, device simulation, dispersion effects, donor traps, drain lag, gate lag, hole traps, surface states, trapping effects.**

I. Introduction

THE GREAT interest raised by AlGaN/GaN high-electron mobility transistors (HEMTs) in the international semiconductor scientific community in general, for high-frequency, high-power, and high-temperature applications, has resulted in that an important number of researchers and centers in the world are nowadays mainly devoted to this new technology. However, there are still some problems in the production of GaN-based devices. The existence of dispersion effects observed in wide-bandgap devices has limited the initial expectations. The considerable list of advantages attributed to devices based on group-III nitrides in the last decade, due to their excellent properties, is partially limited by these negative effects. Great efforts are being dedicated to their understanding and their possible elimination or, at least, minimization.

Manuscript received June 15, 2006; revised December 15, 2006. This work was supported in part by Junta de Comunidades de Castilla-La Mancha under Project PAC-05-001-2 and by Escuela Universitaria de Ingeniería Técnica Industrial (EUITI) de Toledo. The review of this paper was arranged by Editor M. Anwar.

J. M. Tirado is with the Department of Electrical, Electronic, Control and Communications Engineering, University of Castilla-La Mancha, 45071 Toledo, Spain (e-mail: JoseMaria.Tirado@uclm.es).

J. L. Sánchez-Rojas is with the Department of Electrical, Electronic, Control and Communications Engineering, University of Castilla-La Mancha, 13071 Ciudad Real, Spain (e-mail: JoseLuis.SanchezRojas@uclm.es).

J. I. Izpura is with the Department of Electronic Engineering, Universidad Politécnica de Madrid, 28040 Madrid, Spain (e-mail: izpura@die.upm.es).

Digital Object Identifier 10.1109/TED.2006.890592

The presence of trapping centers in FETs based on III–V compounds, related to surface, material, and/or interface states, has been considered as the main cause of these effects [1]–[15], already studied in other technologies. Some of the observed effects are threshold voltage shift [5], [16], current collapse [1], [2], [4], [5], [7]–[9], [11], [12], [14]–[16], reduction of short channel effect [16], light sensitivity [1]–[5], [8], [11], transconductance frequency dispersion [12], [17], gate-lag and drain-lag transients [2], [3], [7], and limited microwave power output [7], [12]. Current collapse—understood as a transient and recoverable reduction in drain–current response—in GaN devices has been associated mainly to the finite time required by surface traps to respond to an external voltage step. Although its origin is under debate, it seems to be induced by process damage—plasma and thermal—which generates nitrogen vacancies [18]. The filling and emptying of traps would change the density of surface charge in the semiconductor and influence the recombination statistics. These parasitic effects, commonly observed in GaN FETs, have been reported by several authors [1]–[6], [11], [13]–[15], [17], and hence, it is very important to include them in physical models in order to fit more exactly the operation of real devices.

In this paper, current collapse is characterized in AlGaN/GaN HEMT by means of pulsed measurements based on gate-lag and drain-lag turn-on techniques. Our measurements suggest that the dispersion effects are characterized by fast time constants—due to surface states—and also, very fast time constants are identified. Two-dimensional numerical device simulations are performed to analyze the influence of surface states on the pulsed characteristics of an AlGaN/GaN HEMT device.

It is demonstrated that the current collapse effect originated from temporary variations in the concentration of donor traps ionized in both regions next to the gate contact (i.e., S–G and also D–G) due to the existence of density of traps lower than the polarization charge and higher depending on the test conditions, mainly when the gate-lag technique is employed.

The activation energy of traps (0.25 eV) is deduced consistently from two experimental techniques by following a fitting procedure through semilogarithmic curves between experimental and theoretical results, obtained from our 2-D physical model.

This paper shows the transient evolution of donor traps ionized and holes at the surface after the transient step voltage is applied, employing the two discussed techniques. It is suggested that the additional fast time constants observed in our results would be related with other mechanisms other than surface states due to the clear transient response obtained also

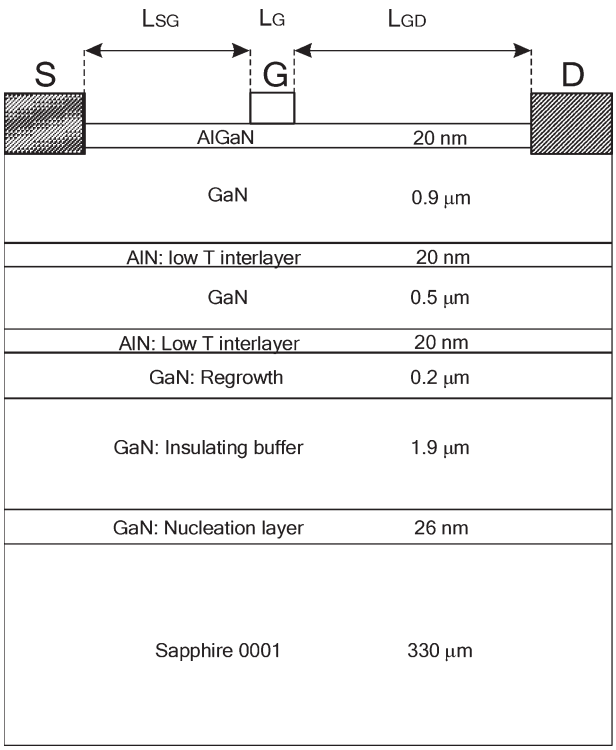

Fig. 1. Schematic cross section of the studied AlGaN–GaN HEMT. Figure not to scale.

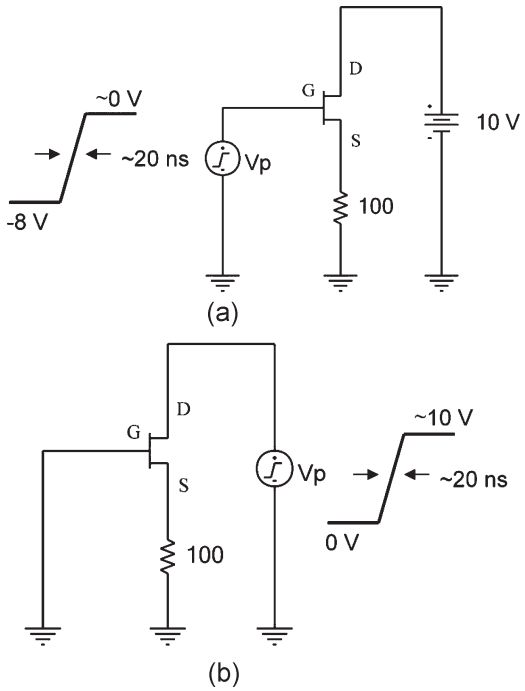

Fig. 2. Experimental set up for the different turn-on pulsed methods. (a) Gate-lag turn-on measurement technique: fixed voltage applied to the drain terminal (10 V), and the gate pulsed from pinchoff to open channel condition (from -8 to 0 V, respectively). (b) Drain-lag turn-on measurement technique: fixed voltage applied to the gate (0 V), and the drain pulsed from OFF-state to open channel condition (from 0 to $\sim +10$ V, respectively).

in this case from our theoretical 2-D model in comparison with experimental results.

Section II is devoted to the analyzed structure and the method of analysis. Section III includes the physical model, the surface state model, and the basic equations employed for the analysis. The theoretical charge model and the nature, density, and energy level of traps are also considered there. In Section IV, a comparison between experimental results and theoretical data obtained by simulation is made. In Section V, the results are discussed and explained in detail with the time evolution and distribution of charges at surface (i.e., ionized traps and holes) when both techniques (i.e., gate lag and drain lag) are employed. Finally, conclusions are included in Section VI.

II. Devices and Experimental Setup

The $Al_{0.36}GaN_{0.64}/GaN$ heterostructure analyzed in this paper is presented in Fig. 1. It was passivated with a 70-nm-thick SiN layer and deposited at 350 °C. It was grown by low-pressure metal–organic vapor phase epitaxy on a c-plane sapphire substrate starting with an undoped 1.9- and 0.2-μm-thick high-resistivity GaN multilayer buffer template, a 0.9-μm-thick GaN top layer, and a 200-Å AlGaN barrier with a composition of 36% in aluminum. In the interlayered buffer heterojunctions, two 20-nm-thick low-temperature AlN layers separated by a 0.5-μm GaN layer were first deposited [19] prior to the growth of the 0.9-μm-thick top buffer and the AlGaN barrier. The gate length is $L_G = 5$ μm, the gate width is $L_W = 75$ μm, and the separation between contacts were $L_{\rm SG} = 1.5$ μm and $L_{\rm GD} = 2$ μm.

In Fig. 2, the widely used gate-lag and drain-lag measurement techniques [2], [3], [7], [16], [20] employed in this paper are presented. In our computational 2-D model, the current sensing resistance used in the measurement circuit is taken into account as part of the source contact resistance.

A. Gate-Lag Turn-On Measurement Technique

A transient voltage step is applied to the gate terminal, maintaining a fixed drain bias of $V_D = 10$ V; the HEMT device is driven under this situation from the initial pinchoff to an open channel condition—$V_{\rm GS} = -8$ V and $\sim$0 V, respectively. The drain–current transient (i.e., gate lag) versus time is registered and analyzed.

B. Drain-Lag Turn-On Measurement Technique

A transient voltage step is applied to the drain terminal, maintaining a fixed gate bias of $V_G = 0$ V; the HEMT device is driven under this situation from the initial OFF-state to an open channel condition—$V_D = 0$ V and $\sim$10 V, respectively. The drain–current transient (i.e., drain lag) versus time is registered and analyzed.

In this paper, a stress drain voltage of $V_{DS} \sim 10$ V is employed in the two techniques. The electrical stress effect on the transient characteristics has been suggested in [21], where the dispersion characteristics are found to be bias dependent, which is associated with the drain bias dependence of trapped carrier concentration. The measurement set up was built by using an Agilent 33250A 80-MHz Function/Arbitrary

Waveform generator for gate and drain pulsing, the pulse rise time in both cases was next to 20–30 ns, and a power supply to maintain $V_D = 10$ V in the first case was employed. An Agilent 54642A digital oscilloscope (two-channel 500-MHz bandwidth, 2 Gsa/s, and MegaZoom technology) is employed to register the excitation signals and the drain response in both cases.

III. Physical Model and Method of Analysis

The 2-D device simulator used in this paper was Silvaco Atlas [22]. Basic equations to be solved are the Poisson equation including the contribution of mobile and fixed charges and ionized traps, the carrier continuity equations for electrons and holes, and the transport equations using the drift-diffusion model. The dynamic traps are modeled by a Shockley–Read–Hall recombination term, included in the continuity equations. An additional differential rate equation is solved to account for emission and capture processes in transient trap simulations. In this paper, carrier lifetimes are controlled by capture cross sections.

The device structure corresponding to the AlGaN/GaN HEMT, modeled and simulated, corresponds to the scheme in Fig. 1 and the same dimensions of the device analyzed in Section II. Various dielectric materials on the surface were considered in the simulations. As expected, the dielectric properties of the layer do not appreciably change our results and conclusions, which certainly depend on the trap parameters considered. The electron GaN mobility measured in the studied heterostructure was next to 1100 $\mathrm{cm}^2/\mathrm{V}\cdot\mathrm{s}$, and this value has also been maintained in our simulation model. The GaN hole mobility assumed in our model was 30 $\mathrm{cm}^2/\mathrm{V}\cdot\mathrm{s}$ [23]. Mobilities of 100 and 5 $\mathrm{cm}^2/\mathrm{V}\cdot\mathrm{s}$ were used in AlGaN for electrons and holes, respectively. Saturation velocities for electron and holes in GaN were taken as vsatn = 1.91e7 cm/s and vsatp = 1e6 cm/s, respectively, according to Monte Carlo fits [22], [24]. Saturation velocities for electron and holes in AlGaN were linearly interpolated from the binaries [22].

The built-in fields due to spontaneous polarization and strain (piezoelectric effect) are taken into account as fixed sheet charges at the AlGaN surface and AlGaN/GaN interface. A positive sheet charge $+\sigma_{\mathrm{pol}}$ with density +1.5e13 cm^{-2} was defined at the interface, and the equivalent negative sheet charge $-\sigma_{\mathrm{pol}}$ was defined at the AlGaN surface. Newton numerical method was used in the models for calculations, and a temperature of 300 K was employed by default in the simulations. Surface states are included through a fixed donor trap density σ_T, uniformly distributed on the regions between source and gate and between gate and drain. A depth of 5 Å [25] is considered, which allows to translate volume densities into sheet densities. This charge is added to the space charge term in Poisson's equation [22]. Although in the analyzed structure a sapphire substrate was employed, and obviously self-heating effects could be a very important aspect to consider as has been suggested by other authors [20], [21], in order to avoid self-heating effects, we have employed a low drain bias ($V_{DS} \sim$ 10 V), and short-time voltage steps were applied to the analyzed device ($\leq$ 10 ms).

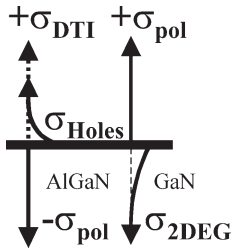

Fig. 3. Scheme of space charge components in a HEMT device considering $\pm\sigma_{\mathrm{pol}}$ (dipole charge due to polarization-induced charges), σ_{2DEG} (charge due to the 2-D electron gas), σ_{holes} (charge due to holes accumulation next to AlGaN surface), and σ_{DTI} (charge due to DTI).

Similar to the experimental test conditions discussed in Section II, a turn-on step voltage ($\leq$ 10 ns) is applied to the gate terminal (from $V_{\mathrm{GS}} = -8$ to 0 V), maintaining a fixed drain bias of $V_D = 10$ V. The drain–current transient (gate lag) versus time is analyzed. Analogously and independently, a turn-on step voltage ($\leq$ 10 ns) is applied to the drain terminal (from $V_{\mathrm{DS}} = 0$ to 10 V), maintaining a fixed gate bias of $V_G = 0$ V. The drain–current transient (drain lag) versus time is also analyzed.

A basic graphical scheme of space charge components in a HEMT device [10], [11], [25] is presented in Fig. 3. Our physical model includes a fixed dipole charge due to polarization-induced charges $-\sigma_{\mathrm{pol}}$ at the AlGaN surface and $+\sigma_{\mathrm{pol}}$ at the AlGaN/GaN interface, charge due to the 2-D electron gas σ_{2DEG} next to the AlGaN/GaN interface, charge due to donor-trap ionization (DTI) σ_{DTI} when donor-type traps are considered at the AlGaN surface, and charge due to holes accumulation next to the AlGaN surface σ_{holes}. Additional sources of charge, due to traps in locations other than the AlGaN surface, such as bulk GaN, AlGaN barrier material, or even AlGaN/GaN interface, have not been included.

The surface states assumed in the model are a key variable since the device response is determined by their magnitude. As shown below, reasonable values, coherent with the measured curves, for the density of donor traps were $\sigma_{T1} = 1.5\mathrm{e}20$ cm^{-3} and $\sigma_{T2} = 3.8\mathrm{e}20$ cm^{-3} by following a fitting procedure to the experimental behavior; the degeneracy factor was 1.0, and capture cross sections of the traps for electrons and holes assumed were $\sigma_n = \sigma_p = 1\mathrm{e}-19$ cm^2; similar orders of magnitude are found in the literature employing sapphire substrates [26]. The energy level of traps employed in our simulations was 0.25 eV, relative to the valence band, as will be discussed in the next section.

IV. Experimental and Numerical Results

In this section, the experimental results obtained by the electrical characterization techniques discussed in Section II are presented. A comparison is also made with numerical simulations, according to the physical model seen in Section III.

A. Gate-Lag Turn-On Pulsing Mode

Fig. 4 shows the drain–current response using the gate-lag technique, as shown in Fig. 2(a). Two different behaviors are

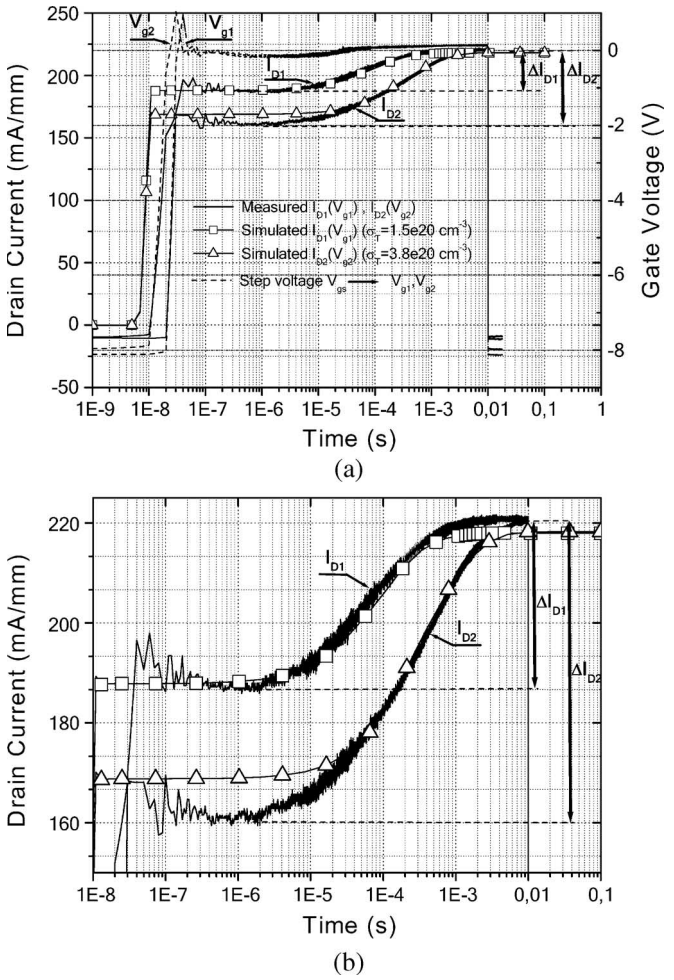

Fig. 4. (a) Experimental and theoretical $I_D(t)$ transient response obtained in an AlGaN/GaN HEMT device using the gate-lag turn-on technique for two test conditions (I_{D1} and I_{D2}) at $V_D = 10$ V. In dashed line is shown the transient step voltages applied to the gate terminal (V_{g1} and V_{g2}). (b) Expanded plot of (a).

identified in the transient response, depending on the relative times involved.

1) In the first case, the device is analyzed starting from an initial situation under relaxed conditions—without electrical excitation applied for at least several minutes. In this situation, a step voltage V_{g1} (dashed line) is applied to the gate terminal—with a rising edge time next to 30 ns. The drain–current registered (gate lag) is presented in the plot as I_{D1} (solid line). As clearly observed, the HEMT device initially presents a fast transition in current response during the first 30 ns, trying to follow with the same edge the evolution of the applied stimulus V_{g1}, as expected. Far from the desirable behavior, an initial decrease in current next to 15% (current collapse)—see arrow labeled as ΔI_{D1} in the plot—is observed. Later on, during a transient evolution, a noticeable increase in current delay is obtained. Current response suffers a lapsed time next to approximately six decades since the step voltage V_{g1} was applied. Finally, a steady-state condition is achieved for $t \geq 10$ ms, maintaining I_{D1} almost constant with time.
2) Also in Fig. 4, a second situation is analyzed. Immediately after several step voltages are applied at the gate terminal, a subsequent step voltage V_{g2} (dashed line) is applied, and the current response registered (I_{D2} curve). In this second case, an initial current collapse next to 27% is observed—see ΔI_{D2} arrow in the plot—with the transient response similar to the previous case. The little differences between V_{g1} and V_{g2} are due to jitter effects in the pulse generator. The differences in the results of the above different excitation conditions are discussed next.

The calculated curves for the transient current responses are also plotted in Fig. 4. By following a fitting procedure in our theoretical model, the two previously analyzed cases are modeled. As shown, considering case 1, both I_{D1} curves, experimental (solid line) and theoretical (squares line), are very similar, predicting our model with remarkable precision the experimental results obtained. Such a good fitting is achieved with a density of traps $\sigma_{T1} = 1.5\text{e}20$ cm^{-3} at the surface and uniformly distributed between contacts; the energy level of traps being 0.25 eV relative to the valence band. The existence of multiple trap levels (≤ 0.25 eV) may well be an acceptable alternative picture, according to our calculations [25].

Considering case 2, the experimental I_{D2} curve (solid line) and the theoretical curve (triangles line) are also very approximated as a result of a new fitting process using our theoretical model, which corresponds to a density of traps next to $\sigma_{T2} = 3.8\text{e}20$ cm^{-3}, for the rest of the conditions being equal to the previous case analyzed. Discussions about the physical mechanism of HEMT response to the stimulus applied are presented in Section V.

B. Drain-Lag Turn-On Pulsing Mode

Fig. 5 shows the transient drain–current using the drain-lag technique, as described in Fig. 2(b). Again, two situations are presented in a similar fashion to the case of excitation in the gate.

1) In the first case, the device is analyzed starting from an initial situation under relaxed conditions—no electrical stress applied for at least several minutes. In this situation, a step drain voltage V_{d1} (dashed line) is applied to the drain terminal (with a rising edge time next to 30 ns), and the drain–current registered (drain lag) is presented in the plot as I_{D1} (solid line). As clearly observed, the device initially shows an instantaneous and maximum peak of current, trying to follow with the same edge the evolution of the applied stimulus V_{d1}, as expected. However, the level of current instantaneously reached (in $\sim$30 ns) has an overshoot next to $\sim$15%, which is over the steady-state value obtained when the gate-lag technique was used. Starting from this point, a decrease—almost linear—of current is observed in curve I_{D1} until a time next to ~ 8 μs (see the t_A label in the expanded plot), where the drain–current seems to be stabilized. After approximately one decade in time, the drain–current starts a less pronounced fall (see the t_B label in the expanded plot) until a steady-state condition for $t \geq 10$ ms is reached again, with the current level very similar to

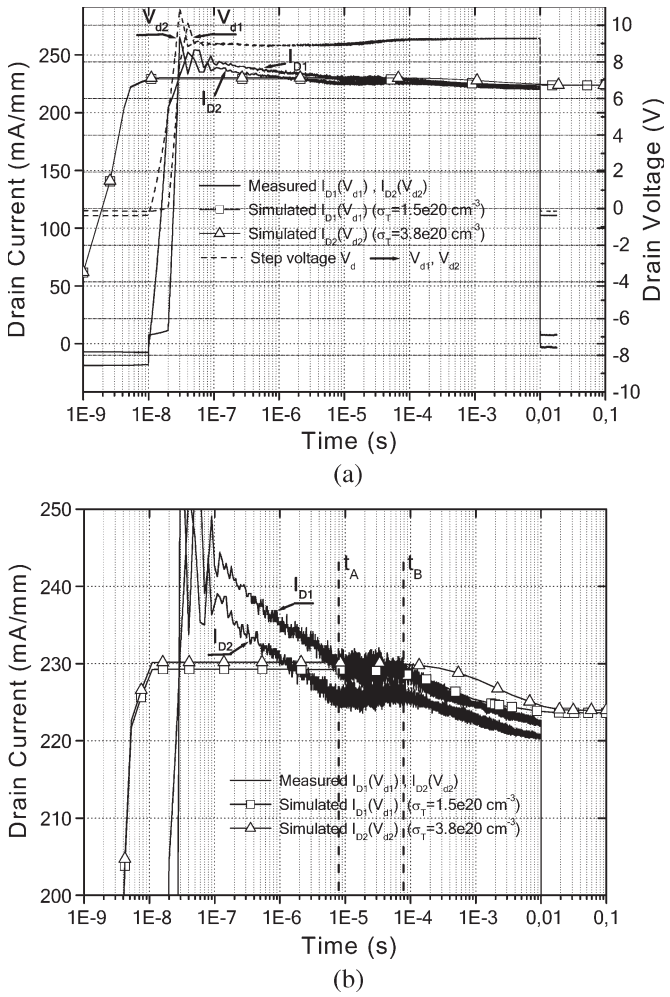

Fig. 5. (a) Experimental and theoretical $I_D(t)$ transient response obtained in an AlGaN/GaN HEMT device using the drain-lag turn-on technique for two test conditions (I_{D1} and I_{D2}) at $V_G = 0$ V. In dashed line is shown the transient step voltages applied to the drain terminal (V_{d1} and V_{d2}). (b) Expanded plot of (a).

that obtained when the gate-lag technique was employed. This particular response will be discussed in the next section.

2) In the second case, a similar procedure was followed using electrical stress conditions. Several step voltages are applied at the drain terminal, a subsequent step voltage V_{d2} (dashed lined) is registered, and the current response is analyzed. However, unlike the gate-lag technique previously discussed, lower differences were obtained with respect to case 1 using this second technique. Hence, in this case, we represent in Fig. 5 only the maximum variations observed in our tests: curve I_{D2} (solid line). Although due to the scale used it is not directly appreciated, the average variation in current level in the last decade, in both curves, was lower than 3 mA/mm.

In Fig. 5, the numerical results using the drain-lag technique are also presented for the two situations considered, analogous to the gate-lag technique previously described and also employing the same physical model. The densities of donor traps assumed in our simulations were again $\sigma_{T1} = 1.5\text{e}20$ cm^{-3} (squares line) and $\sigma_{T2} = 3.8\text{e}20$ cm^{-3} (triangles line). As can

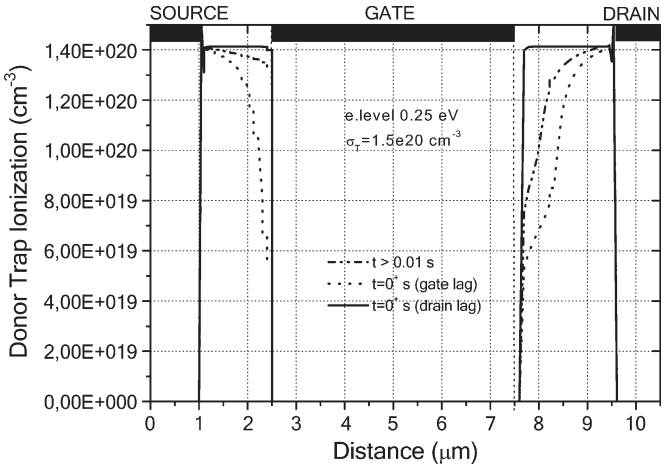

Fig. 6. DTI concentration in horizontal cut made at the HEMT surface for $t = 0^+$ s (gate lag, dashed line; and drain lag, solid line) and for $t > 10$ ms (dash-dotted line) in both cases.

be observed in the figure, the current deviations between the two simulated curves are minimal, and similar time constants are obtained in both cases, with a delay of approximately two decades—from $\sim$80 μs (t_B) to 10 ms—see expanded plot in Fig. 5(b).

V. Discussion

In this section, the results shown in Section IV and presented in Figs. 4 and 5 are compared and discussed, describing our physical explanation to the HEMT behavior.

A. Gate-Lag Results

The initial current collapse situation observed in Fig. 4 was directly caused by a significant amount of neutral donor states at the surface, filled with electrons. The surface states in the form of DTI ($\sigma_{\rm DTI}$) contribute by adding a positive charge to the net total, expressed as $\sigma_{\rm net} = -\sigma_{\rm pol} + \sigma_{\rm DTI} + \sigma_{\rm holes}$ [25]. According to our charge model seen in Fig. 3, $\sigma_{\rm DTI}$ would have the lowest positive value. These effects of reduction of negative charges at the surface on the drain–current, under static conditions, were reported in [27], producing an opposite response to the classical behavior of a GaN-based MESFET device [28]. With minimum $\sigma_{\rm DTI}$, the initial response of the device in drain–current has the minimum level, i.e., a "collapsed" situation in current is observed in the device under our experimental test conditions. This is clearly shown in Fig. 6, where the DTI concentration, just after application of the step gate voltage, is represented [$t = 0^+$ s (dashed line)]. Another important source of positive charge to consider would be free holes that accumulated at the surface, as plotted in Fig. 7. The hole concentration at the surface $\sigma_{\rm holes}$ is given just after the step voltage was applied $t = 0^+$ s (dashed line). As reported in [25], its magnitude is very dependent on the energy level of traps. However, the contribution of holes to the net charge $\sigma_{\rm net}$, when donor states are included in the model, is minimal in all cases and does not have an important influence as positive charge.

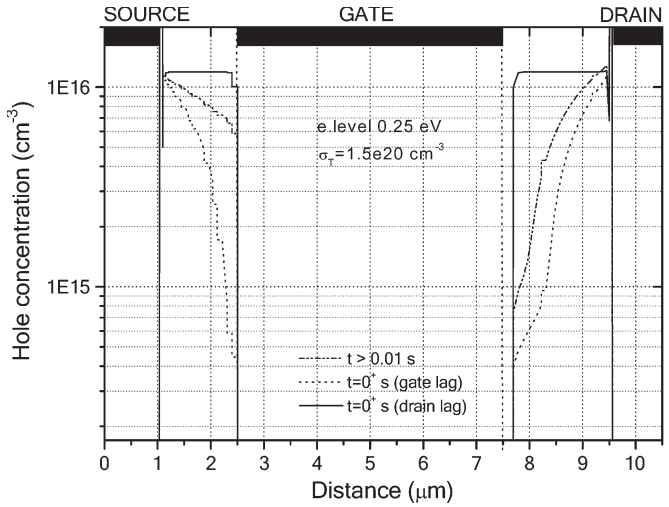

Fig. 7. Hole concentration in horizontal cut made at the HEMT surface for $t = 0^+$ s (gate lag, dashed line; and drain lag, solid line) and for $t > 10$ ms (dash-dotted line) in both cases.

Later on, the finite time required by surface states to respond to the external gate voltage step (V_{g1} or V_{g2}) would be the cause of the lapsed time observed in Fig. 4. As reported in [25], time constants are very dependent on the energy level of traps.

The increase of DTI with time at the surface—by emission of electrons or capture of holes—would be the direct origin of the transient evolution of current observed in curves I_{D1} and I_{D2}. In our case, the capturing of holes seems to be the most reasonable because, as reported in [25], donor traps at the surface would be close to free holes that accumulated at the HEMT surface—due to piezo effects—making it very likely the process of capturing holes by donor traps. As deduced from [25] and according to [29] for energy of traps below Fermi level at equilibrium, traps would be essentially full or substantially filled with holes as it is this case, the lower is the energy level of traps, the greater is the probability that traps act as hole traps instead of recombination centers. Fig. 6 shows the DTI concentration for $t \geq 10$ ms when a steady-state condition has been achieved (dash-dotted line). The temporary variation suffered by DTI and how this variation is greater in regions next to the gate contact and lower in regions next to the source and drain contacts are clear and evident. Therefore, this mechanism is mainly responsible for the effect of current collapse in AlGaN/GaN HEMTs, i.e., variations of charge at the surface next to the gate contact, independent of the existence of traps in another material location and/or interface. The bias conditions would determine the relative position of quasi-Fermi level for trapped holes with respect to the energy level of traps and consequently their degree of ionization. In Fig. 7, the variation experienced by the hole concentration for $t \geq 10$ ms (dash-dotted line), following a similar behavior to the variation of DTI described, is also shown.

The very low influence of acceptor traps at the surface of our device—acting as electron traps—has also been reported in [25]. Another important aspect to add in these conclusions is a fact already reported in the literature [20]: it seems that no other source of traps—GaN, AlGaN material, or AlGaN/GaN interface—was detected in our measurements employing the described technique.

The last aspect to be discussed at this point would be in connection to the number of active traps at the surface. As revealed by our results considering the two excitation conditions seen in Section IV-A, the number of active traps at the surface would depend on the electrical history suffered by the device.

B. Drain-Lag Results

From the drain-lag turn-on measurements shown in Fig. 5, analyzing the interval between $t > 0$ and $t < t_A$ [Fig. 5(b)], the transient decrease in current is not due, according to our simulations, to the presence of surface states, because a slower behavior and similar to the gate-lag case could be expected, and trapping centers in other locations, such as bulk GaN, AlGaN, and/or interface, are likely. At the present state of our investigations, we cannot give the exact origin of these observed effects. But in this case, a very fast response with time constants next to $\sim$10 μs—see t_A in the expanded plot—is identified. On the other hand, analyzing the interval for $t \geq t_A$, we identify the presence of fast donor surface traps in the current response with the associated time constants next to 10 ms—analogous to gate-lag measurements. Unlike the explanation given in case A, where current collapse was due to neutral donor traps filled with electrons, in this case, the behavior of traps at the surface would be the opposite. Considering $0 < t < t_B$, initially, most of the traps are emptied and positively charged—electrons have been emitted or holes captured. This last situation seems to be more reasonable, according to our previous discussion. In Fig. 6, the DTI concentration, just after the drain step voltage was applied [$t = 0^+$ s (solid line)], is shown. The concentration of DTI is greater than in the previous case. The contribution of surface states σ_{DTI} adding positive charge to the net charge at the surface σ_{net} would be maximum for $t < t_B$ in Fig. 5(b). Later on, during the transient evolution, for $t \geq t_B$, the finite time required by surface traps to respond to the external voltage step (V_{d1} or V_{d2}) would be again the cause of this effect by a process of filling and subsequent neutralization—electrons captured or holes emitted. The decrease of DTI at the surface would be the direct cause of the transient evolution of current observed in the curves shown in Fig. 5. In this case, a decrease of positive charge σ_{DTI} is associated with the filling and neutralizing of positive donor traps by capture of electrons or emission of holes. In our case again, the emission of holes seems to be the most reasonable according the explanation given in Section V-A. In Fig. 6, the DTI concentration for $t \geq 10$ ms (dash-dotted line), when a steady-state condition has been achieved, is also presented. The DTI concentration agrees with the result obtained in case A. In this second case, a decrease of DTI concentration is observed in the regions next to the gate contact. In Fig. 7, the hole concentration for $t \geq 10$ ms (dash-dotted line) is shown for the same conditions, in agreement with the results obtained in case A.

As a conclusion to this section, our model accounts for all the features measured in the current response both in gate and drain pulse excitation, except for the initial and fast decrease

of drain–current in the second case that would be related with other mechanisms than surface states.

In both analyzed responses, the mutual interaction between free holes that accumulated at the HEMT surface and donor traps turns out to be decisive in this particular behavior of AlGaN/GaN HEMT, unlike classical GaN MESFET behavior [25]. Holes and donor states play a decisive and very important electrostatic role on the physical mechanism of response of 2DEG in AlGaN/GaN HEMT and consequently in the variation of drain–current response in the device.

Finally, it is worth emphasizing that both gate and drain pulses lead to the same final steady-state condition in current response in a HEMT device, i.e., such mechanism is due to the contribution—increment or decrement—of positive charge, caused by the DTI σ_{DTI}, to the net charge σ_{net} in the regions next to the gate contact, leading to the same steady-state condition in a HEMT device, because the final DTI concentration at the surface σ_{DTI}—for $t \geq 10$ ms—is the same in both cases; and as a result, the same level in current response is achieved when steady-state conditions are reached.

VI. Conclusion

In this paper, we have presented the trapping effects in the transient response of a HEMT device. The mechanism of drain current changes in the device has been analyzed by comparing experimental and calculated currents. We have demonstrated the existence of current collapse and related dispersion effects, employing an analysis based on the well-known techniques of gate-lag and drain-lag turn-on pulsing methods, and discussing their effects. These techniques have verified the model of donor surface states—acting as hole traps—being mainly responsible for the observed negative effects in this technology. Besides, the existence of additional sources of dispersion not associated with surface states has been deduced. A HEMT physical model has been studied to explain the experimental results, and the structure has been analyzed by means of a 2-D device simulator that includes time evolution of trap ionization. Donor states with an energy level of 0.25 eV—relative to the valence band—and densities in the range of 1.5e20–3.8e20 cm^{-3}, located at the ungated surface, and interacting with free holes that accumulated at the surface due to piezo effects, between contacts, would be the source of the current collapse effects; this is consistent with the time evolution of DTI concentration at the surface. Theoretical DTI evolution has been shown and described using the two discussed techniques, and time constants next to 10 ms have been obtained in both experimental and theoretical results. Experimental time constants next to 10 μs that have also been measured in the drain–current pulses may be associated with sources of trapping in locations other than the surface.

Acknowledgment

The authors would like to thank F. Garat of ESA-ESTEC for valuable discussions and suggestions, the Microsystems Laboratory, Universidad Politécnica de Madrid, for the use of clean room facilities, and Prof. E. Iborra and Prof. J. Sangrador for the assistance.

References

[1] M. A. Khan, M. S. Shur, Q. C. Chen, and J. N. Kuznia, "Current–voltage characteristic collapse in AlGaN/GaN heterostructure insulated gate field effect transistors at high drain bias," *Electron. Lett.*, vol. 30, no. 25, pp. 2175–2176, Dec. 1994.

[2] S. C. Binari, W. Kruppa, H. B. Dietrich, G. Kelner, A. E. Wickenden, and J. A. Freitas, "Fabrication and characterization of GaN FETs," *Solid State Electron.*, vol. 41, no. 10, pp. 1549–1554, Oct. 1997.

[3] S. Trassaert, B. Boudart, C. Gaquiére, Y. Théron, Y. Crosnier, F. Huet, and M. A. Poisson, "Trap effects studies in GaN MESFETs by pulsed measurements," *Electron. Lett.*, vol. 35, no. 16, pp. 1386–1388, Aug. 1999.

[4] P. B. Klein, J. A. Freitas, S. C. Binari, and A. E. Wickenden, "Observation of deep traps responsible for current collapse in GaN metal–semiconductor field-effect transistors," *Appl. Phys. Lett.*, vol. 75, no. 25, pp. 4016–4018, Dec. 1999.

[5] G. Meneghesso, A. Chini, E. Zanoni, M. Manfredi, M. Pavesi, B. Boudart, and C. Gaquiere, "Diagnosis of trapping phenomena in GaN MESFETs," in *IEDM Tech. Dig.*, Dec. 2000, pp. 389–392.

[6] I. Daumiller, D. Theron, C. Gaquière, A. Vescan, R. Dietrich, A. Wieszt, H. Leier, R. Vetury, U. K. Mishra, I. P. Smorchkova, S. Keller, N. X. Nguyen, C. Nguyen, and E. Kohn, "Current instabilities in GaN-based devices," *IEEE Electron Device Lett.*, vol. 22, no. 2, pp. 62–64, Feb. 2001.

[7] S. C. Binari, K. Ikossi, J. A. Roussos, W. Kruppa, D. Park, H. B. Dietrich, D. D. Koleske, A. E. Wickenden, and R. L. Henry, "Trapping effects and microwave power performance in AlGaN/GaN HEMTs," *IEEE Trans. Electron Devices*, vol. 48, no. 3, pp. 465–471, Mar. 2001.

[8] P. B. Klein, S. C. Binari, K. Ikossi-Anastasiou, A. E. Wickenden, D. D. Koleske, R. L. Henry, and D. S. Katzer, "Investigation of traps producing current collapse in AlGaN/GaN high electron mobility transistors," *Electron. Lett.*, vol. 37, no. 10, pp. 661–662, May 2001.

[9] P. B. Klein, S. C. Binari, K. Ikossi, A. E. Wickenden, D. D. Koleske, and R. L. Henry, "Current collapse and the role of carbon in AlGaN/GaN high electron mobility transistors grown by metalorganic vapor-phase epitaxy," *Appl. Phys. Lett.*, vol. 79, no. 21, pp. 3527–3529, Nov. 2001.

[10] J. P. Ibbetson, P. T. Fini, K. D. Ness, S. P. DenBaars, J. S. Speck, and U. K. Mishra, "Polarization effects, surface states, and the source of electrons in AlGaN/GaN heterostructure field effect transistors," *Appl. Phys. Lett.*, vol. 77, no. 2, pp. 250–252, Jul. 2000.

[11] R. Vetury, N. Q. Zhang, S. Keller, and U. K. Mishra, "The impact of surface states on the DC and RF characteristics of AlGaN/GaN HFETs," *IEEE Trans. Electron Devices*, vol. 48, no. 3, pp. 560–566, Mar. 2001.

[12] S. C. Binari, P. B. Klein, and T. E. Kazior, "Trapping effects in GaN and SiC microwave FETs," *Proc. IEEE*, vol. 90, no. 6, pp. 1048–1058, Jun. 2002.

[13] R. J. Trew, "SiC and GaN transistors—Is there one winner for microwave power applications?" *Proc. IEEE*, vol. 90, no. 6, pp. 1032–1047, Jun. 2002.

[14] J. I. Izpura, "Drain–current collapse in GaN metal–semiconductor field-effect transistors due to surface band-bending effects," *Semicond. Sci. Technol.*, vol. 17, no. 12, pp. 1293–1301, Dec. 2002.

[15] G. Verzellesi, R. Pierobon, F. Rampazzo, G. Meneghesso, A. Chini, U. K. Mishra, C. Canali, and E. Zanoni, "Experimental/numerical investigation on current collapse in AlGaN/GaN HEMT's," in *IEDM Tech. Dig.*, Dec. 2002, pp. 689–692.

[16] Y. Hasumi and H. Kodera, "Simulation of the surface trap effect on the gate lag in GaAs MESFETs," *Electron. Commun. Jpn.*, vol. 85, no. 2, pp. 18–26, 2002.

[17] W. Kruppa, S. C. Binari, and K. Dovespike, "Low-frequency dispersion characteristics of GaN HFETs," *Electron. Lett.*, vol. 31, no. 22, pp. 1951–1952, Oct. 1995.

[18] W. Saito, M. Kuraguchi, Y. Takada, K. Tsuda, I. Omura, and T. Omura, "Influence of surface defect charge at AlGaN/GaN-HEMT upon Schottky gate leakage current and breakdown voltage," *IEEE Trans. Electron Devices*, vol. 52, no. 2, pp. 159–164, Feb. 2005.

[19] Z. Bougrioua, I. Moerman, L. Nistor, B. Van Daele, E. Monroy, T. Palacios, F. Calle, and M. Leroux, "Engineering of an insulating buffer and use of AlN interlayers: Two optimisations for AlGaN-GaN HEMT-like structures," *Phys. Stat. Sol. A*, vol. 195, no. 1, pp. 93–100, Jan. 2003.

[20] G. Meneghesso, G. Verzellesi, R. Pierobon, F. Rampazzo, A. Chini, U. K. Mishra, C. Canali, and E. Zanoni, "Surface-related drain–current dispersion effects in AlGaN-GaN HEMTs," *IEEE Trans. Electron Devices*, vol. 51, no. 10, pp. 1554–1561, Oct. 2004.

[21] S. S. Islam, A. F. M. Anwar, and R. T. Webster, "A physics-based frequency dispersion model of GaN MESFETs," *IEEE Trans. Electron Devices*, vol. 51, no. 6, pp. 846–853, Jun. 2004.

[22] *Device Simulator Atlas Ver. 5.10.0.R. Atlas User's Manual*, Silvaco Int., Santa Clara, CA, Jul. 2005.
[23] S. J. Pearton, F. Ren, A. P. Zhang, and K. P. Lee, "Fabrication and performance of GaN electronic devices," *Mater. Sci. Eng.*, vol. 30, no. 3–6, pp. 55–212, Dec. 2000.
[24] M. Farahmand, C. Garetto, E. Bellotti, K. F. Brennan, M. Goano, E. Ghillino, G. Ghione, J. D. Albrecht, and P. P. Ruden, "Monte Carlo simulation of electron transport in the III-nitride Wurtzite phase materials system: Binaries and ternaries," *IEEE Trans. Electron Devices*, vol. 48, no. 3, pp. 535–542, Mar. 2001.
[25] J. M. Tirado, J. L. Sanchez-Rojas, and J. I. Izpura, "Simulation of surface states effects in the transient response of AlGaN/GaN HEMT and GaN MESFET devices," *Semicond. Sci. Technol.*, vol. 21, no. 8, pp. 1150–1159, Jul. 2006.
[26] N. Sghaier, M. Trabelsi, N. Yacoubi, J. M. Bluet, A. Souifi, G. Guillot, C. Gaquière, and J. C. DeJaeger, "Traps centers and deep defects contribution in current instabilities for AlGaN/GaN HEMT's on silicon and sapphire substrates," *Microelectron. J.*, vol. 37, no. 4, pp. 363–370, May 2005.
[27] J. M. Tirado, J. L. Sanchez-Rojas, and J. I. Izpura, "2-D simulation of static surface states in AlGaN/GaN HEMT and GaN MESFET devices," *Semicond. Sci. Technol.*, vol. 20, no. 8, pp. 864–869, Jul. 2005.
[28] ——, "Numerical 2-D simulation of surface states effects in AlGaN/GaN HEMT and GaN MESFET devices," in *Proc. IEEE 5th. Conf. Nanotechnol.*, Jul. 2005, vol. 2, pp. 531–532.
[29] J. G. Simmons and G. W. Taylor, "Nonequilibrium steady-state statistics and associated effects for insulators and semiconductors containing an arbitrary distribution of traps," *Phys. Rev. B, Condens. Matter*, vol. 4, no. 2, pp. 502–511, Jul. 1971.

José María Tirado was born in Madrigal de la Vera, Cáceres, Spain, in 1972. He received the B.Sc. degree in telecommunication engineering from the University of Alcalá de Henares, Madrid, Spain, in 1995, and the M.Sc. degree in telecommunication engineering from the Universidad Politécnica de Madrid, in 2000. He is currently working toward the Ph.D. degree in electronic engineering at the University of Castilla-La Mancha, Toledo, Spain.

From 2000 to 2001, he was an Associate Professor of material engineering with the Universidad Politécnica de Madrid. From 2001 to 2003, he was an Associate Professor of telecommunications engineering with the Universidad Politécnica de Madrid, where he worked in the fabrication and characterization of AlGaN/GaN HEMTs for high-power and high-frequency applications. Since 2003, he has been an Assistant Professor of electronic engineering with the University of Castilla-La Mancha. His research focuses on GaN-based FET devices for microwave and power applications, characterization, and modeling.

José Luis Sánchez-Rojas received the B.E., M.S., and Ph.D. degrees in telecommunication engineering from Universidad Politécnica de Madrid, Madrid, Spain.

In 1997, he was an Invited Postdoctoral Scientist with Cornell University, Ithaca, NY, and Colorado University, Boulder. He is currently a Professor with the University of Castilla-La Mancha, Ciudad Real, Spain. He was a Principal Investigator or task leader in various international projects: ESPRIT 2035 (GIANTS), ESPRIT 3086 (Strained semiconductors), ESPRIT LTR35112 (GHISO Lasers), and NICOP Office of Naval Research project on IR detectors. He is also a Project Reviewer for the European Community. He has been involved in quantum heterostructures since 1991. He is also the author or coauthor of more than 50 papers in this field. His research interests cover optical and electrical characterization and modeling of semiconductor nanostructures and biomolecular devices.

Dr. Sánchez-Rojas achieved the Extraordinary Award of Doctorate granted to a number of high-quality Ph.D. theses in 1995. In 1996, he received the Annual Award of the Universidad Politécnica de Madrid to the Best Young Researcher (under 35).

José Ignacio Izpura was born in Zaragoza, Spain, in 1960. He received the Telecommunication Engineer and Ph.D. degrees from the Telecommunication Engineering School, Universidad Politécnica de Madrid (UPM), Madrid, Spain, in 1983 and 1989, respectively.

Since 1991, he has been an Adjunct Professor with the Department of Electronic Engineering, UPM. From 1984 to 1993, he was engaged in research on AlGaAs/GaAs-based heterojunction bipolar transistors and resonant tunneling diodes. Since 1993, he has been involved in quantum-well-based optoelectronic devices, as InGaAs/GaAs QW lasers on $\langle 111 \rangle$ B GaAs substrates to obtain strained-induced piezoelectric benefits. He has carried out several related projects, such as the ESPRIT-35112 one that he coordinated. His current research activities cover electronic and optoelectronic characterization of devices and microsensors with special interest in the origin and measurement of excess noise.